Biochimica et Biophysica Acta 1848 (2015) 315–322

Contents lists available at ScienceDirect

Biochimica et Biophysica Acta

journal homepage: www.elsevier.com/locate/bbamem

Effects of naturally occurring arginine 14 deletion on phospholamban conformational dynamics and membrane interactions☆,☆☆

Vitaly V. Vostrikov [a,1], Kailey J. Soller [b,1], Kim N. Ha [a,c], T. Gopinath [a], Gianluigi Veglia [a,b,*]

[a] Department of Biochemistry, Molecular Biology and Biophysics, University of Minnesota, Minneapolis, MN 55455, USA
[b] Department of Chemistry, University of Minnesota, Minneapolis, MN 55455, USA
[c] Department of Chemistry and Biochemistry, St. Catherine University, St. Paul, MN 55105, USA

ARTICLE INFO

Article history:
Received 30 June 2014
Received in revised form 12 September 2014
Accepted 13 September 2014
Available online 22 September 2014

Keywords:
Phospholamban
R14 deletion
Solid-state NMR
Membrane proteins
SERCA
Dilated cardiomyopathy

ABSTRACT

Phospholamban (PLN) is a single-pass membrane protein that regulates the sarco(endo)plasmic reticulum Ca^{2+}-ATPase (SERCA). Phosphorylation of PLN at Ser16 reverses its inhibitory function under β-adrenergic stimulation, augmenting Ca^{2+} uptake in the sarcoplasmic reticulum and muscle contractility. PLN exists in two conformations; a T state, where the cytoplasmic domain is helical and adsorbed on the membrane surface, and an R state, where the cytoplasmic domain is unfolded and membrane detached. Previous studies have shown that the PLN conformational equilibrium is crucial to SERCA regulation. Here, we used a combination of solution and solid-state NMR to compare the structural topology and conformational dynamics of monomeric PLN (PLN^{AFA}) with that of the PLN^{R14del}, a naturally occurring deletion mutant that is linked to the progression of dilated cardiomyopathy. We found that the behavior of the inhibitory transmembrane domain of PLN^{R14del} is similar to that of the native sequence. Conversely, the conformational dynamics of R14del both in micelles and lipid membranes are enhanced. We conclude that the deletion of Arg14 in the cytoplasmic region weakens the interactions with the membrane and shifts the conformational equilibrium of PLN toward the disordered R state. This conformational transition is correlated with the loss-of-function character of this mutant and is corroborated by SERCA's activity assays. These findings support our hypothesis that SERCA function is fine-tuned by PLN conformational dynamics and begin to explain the aberrant regulation of SERCA by the R14del mutant. This article is part of a Special Issue entitled: NMR Spectroscopy for Atomistic Views of Biomembranes and Cell Surfaces. Guest Editors: Lynette Cegelski and David P. Weliky.

1. Introduction

Calcium transport in the heart muscle is orchestrated by several different membrane proteins. In particular, the uptake of Ca^{2+} ions into the sarcoplasmic reticulum (SR) is governed by a membrane protein complex between the sarco(endo)plasmic reticulum Ca^{2+}-ATPase (SERCA) and phospholamban (PLN) [1–3]. This complex is responsible for about 70% of the Ca^{2+} transport into the SR in humans. The paramount importance of the SERCA/PLN complex stems from its direct involvement in the cardiac output [4]. Dysfunctions in Ca^{2+} handling by this membrane protein complex lead to the progression of several cardiomyopathies with eventual development of heart failure [5]. To date, several different mutations of the *pln* gene have been sequenced and identified in humans who develop hereditary cardiomyopathies. Among those, a mutation in the *pln* promoter, a truncation resulting in a $PLN^{L39stop}$ mutant, aberrant R9C, R9L, and R9H mutations, as well as *pln* gene duplications, have been directly linked to either dilated or hypertrophic cardiomyopathy [6–9]. Additionally, a recurring deletion of arginine 14 (R14del) in the regulatory domain of PLN was first observed only in heterozygous patients suffering from dilated cardiomyopathy (DCM), a disorder of the heart manifested as enlargement of the left ventricle [8]. Subsequent genetic screening studies of a wider population, broadened the impact of this PLN mutant, not only identifying the Arg14 deletion in patients diagnosed with dilated cardiomyopathy, but also in those with arrhythmogenic right ventricular cardiomyopathy [10].

Powered by ATP, SERCA translocates two Ca^{2+} ions into the SR in exchange for three H_3O^+ ions. It is reversibly inhibited by PLN, a 52 amino acid single-pass membrane protein [11]. PLN exists as a pinwheel-

Abbreviations: DCM, dilated cardiomyopathy; LOF, loss of function; PKA, protein kinase A; PLN^{AFA}, phospholamban monomer bearing mutations C36A C41F C46A; PLN^{WT}, wild type phospholamban pentamer; pSer, phosphoserine; SERCA, sarco(endo)plasmic reticulum Ca^{2+} ATPase; R14del, phospholamban mutant lacking arginine in position 14; SE-PISEMA, sensitivity enhanced polarization inversion spin exchange at magic angle; SR, sarcoplasmic reticulum; TM, transmembrane

☆ This article is part of a Special Issue entitled: NMR Spectroscopy for Atomistic Views of Biomembranes and Cell Surfaces. Guest Editors: Lynette Cegelski and David P. Weliky.

☆☆ This work was supported by the National Institute of Health (GM072701).

* Corresponding author at: Gianluigi Veglia, 321 Church St. SE, Jackson Hall, 6-155, University of Minnesota, Minneapolis, MN 55455, USA. Tel.: +1 612 625 0758; fax: +1 612 625 2163.
E-mail address: vegli001@umn.edu (G. Veglia).

[1] These authors contributed equally to the work.

http://dx.doi.org/10.1016/j.bbamem.2014.09.007
0005-2736/

shaped pentamer, with the inhibitory region comprised of the transmembrane domain II and more hydrophilic domain Ib crossing the lipid membrane with a ~15–20° tilt angle [12–14]. The transmembrane domains of the protomers are arranged in a left-handed coiled-coil of approximately 40 Å in length. In the ground state, the cytoplasmic, regulatory region (loop and domain Ia) is adsorbed on the membrane surface. This interaction is stabilized by the energetically favorable contacts between the aliphatic residues of the domain Ia helix with the hydrophobic core of the membrane, as well as the electrostatic interactions of the polar residues with the lipid head groups and the bulk solvent. Mutagenesis and biophysical data have lead to a regulatory model in which de-oligomerized PLN forms a 1:1 inhibitory complex with the ATPase [11,15]. Following phosphorylation at Ser16 by protein kinase A (PKA), PLN inhibition is negated and Ca^{2+} flux in the SR is augmented. This model was recently confirmed by three different crystal structures obtained with PLN and its homologous analog sarcolipin (SLN) in complex with SERCA [16–18]. The inhibitory domains of the two proteins (i.e., the transmembrane domain II for PLN) bind in a hydrophobic groove between TM2 and TM9 of the ATPase. However, the scarce resolution of electron density for the cytoplasmic domain of PLN did not enable the clarification of the molecular details of its regulatory mechanism.

In the past years we have used NMR spectroscopy to determine PLN structures free and bound to SERCA [13,19,20]. Based on our studies, we proposed a regulatory model in which PLN conformational equilibrium is central to SERCA regulation. We found that PLN exists in three main states: a ground state (T state) with the cytoplasmic domain adsorbed on the surface of the lipid membrane, an excited state (R state), where the cytoplasmic domain is unfolded and membrane detached, and a SERCA bound state (B state), where the transmembrane domain of PLN is bound to SERCA and the extended domain Ia interacts with SERCA's cytoplasmic domains [21–23]. Phosphorylation at Ser16 shifts the equilibrium toward the B state with a local structural rearrangement [19]. The existence of the different PLN structural states is corroborated by mutagenesis studies, demonstrating that it is possible to promote the R and B states with concomitant relief of SERCA inhibition [24].

Here, we investigated how the alteration of the conserved amphipathic motif via a naturally occurring amino acid deletion in the cytoplasmic domain affects PLN conformational equilibrium and its regulation of SERCA. Challenges associated with studying membrane proteins called for a combination of solution and solid-state NMR experiments [25]. We found that the deletion of Arg14 slightly alters the transmembrane domain of the protein, as well as induces a pronounced shift of the conformational equilibrium of the cytoplasmic domain toward the membrane-detached R state. Furthermore, we found that in contrast with PLN, synthetic phosphorylation of PLN^{R14del} does not relieve inhibition of SERCA. This suggests that the PLN^{R14del} mutant functions as a constant inhibitor of SERCA, unresponsive to typical regulatory mechanisms like β-adrenergic stimulation. Analyzing these data with the dynamic ruler we developed for site specific mutants of PLN, our data begins to rationalize the loss-of-function nature of R14del and how it influences not only Ca^{2+} transport in the SR but also the development of cardiomyopathies for individuals carrying this mutation.

2. Material and methods

2.1. Protein production

Phospholamban with a deletion of Arg14 was produced from PLN^{AFA} by site-directed mutagenesis, using QuikChange kit (Stratagene, La Jolla, CA). Expression and purification steps were identical to the host sequence [26]. Briefly, the construct was expressed with R14del fused with maltose binding protein via a tobacco etch virus protease cleavage site. Fusion protein was purified by affinity chromatography on amylose resin, and upon cleavage — by high performance liquid chromatography. To produce Ser16 phosphorylated R14del for the activity assays, we have employed microwave assisted solid phase peptide synthesis as described previously, using Fmoc-Ser[PO(OBzl)] (Merck, Darmstadt, Germany). Phosphoserine was coupled at 50 °C; subsequent deprotection steps were performed at room temperature and amino acids 1–15 were coupled at 50 °C to reduce the risk of dephosphorylation. SDS-PAGE of Ser16-phosphorylated R14del is shown in Supplementary Fig. 1.

2.2. Nuclear magnetic resonance

Solution NMR was performed as described previously. Phospholamban was reconstituted in dodecylphosphocholine-d_{38} and the relaxation measurements were performed at 600 MHz proton frequency on a Varian spectrometer [27]. Separated local field experiments were performed on R14del reconstituted in DMPC:POPC 4:1 bicelles, doped with 1% (mol) DMPE-PEG350 and 1% (mol) PE-DTPA to promote ytterbium ion chelation. Protein was reconstituted in long chained lipids, followed by the addition of the capping lipid (1,2-dihexanoyl-*sn*-glycero-3-phosphocholine; DHPC) [28]. The q-ratio (total long chained lipid to short chained lipid) was 4.5. To promote the parallel orientation of the bicelles $YbCl_3$ was added to the final concentration of 8 mM [29]. The ^{15}N–^{1}H SE-PISEMA experiment was performed on uniformly labeled ^{15}N PLN at 700 MHz on a Varian spectrometer. Magic angle spinning experiments were recorded on uniformly labeled $^{13}C/^{15}N$ PLN in DMPC-d_{54}. Multilamellar vesicles containing PLN were pelleted down overnight at 250,000 g; the pellet was transferred into a Bruker 22 μl rotor and additional buffer was added to ensure that the sample retains hydration throughout the experiment. Refocused INEPT ^{13}C–^{1}H spectra were recorded at 10 kHz spinning rate on a 700 MHz spectrometer.

2.3. SERCA ATPase assays

SERCA1a was extracted from rabbit skeletal muscle and purified using affinity chromatography using previously described methods [30]. SERCA1a and PLN were co-reconstituted in 1,2-dioleoyl-*sn*-glycero-3-phosphocholine: 1,2-dioleoyl-*sn*-phosphoethanolamine (Avanti, Alabaster, AL) at a 4:1 molar ratio in lipid vesicles as previously described [31]. Molar ratios of 10:1 PLN:SERCA and 700:1 lipids:SERCA were used. The Ca^{2+} dependence of SERCA's ATPase activity was measured spectrophotometrically with a Spectromax microplate reader (Molecular Devices) as a function of NADH consumption using coupled enzyme assays at 37 °C as previously described [32,33]. Solutions were equilibrated at 37 °C before the experiment and reaction plate was incubated at 37 °C for 20 min before reaction initiation. The initial rate of ATPase activity (V) was measured as a function of calcium concentration and the data were fit using a standard Hill equation:

$$V = \frac{V_{max}}{1 + 10^{n(pK_{Ca} - pCa)}}$$

where V is the initial rate of ATPase activity, V_{max} is the maximal rate, n is the Hill coefficient, pCa is the log of the Ca^{2+} concentration, and pK_{Ca} is the pCa value where $V = V_{max} / 2$.

The assays were performed with three separate reconstitutions, with triplicate measurements for each separate reconstitution.

3. Results

3.1. SERCA ATPase assays

Haghighi and coworkers found that PLN^{R14del} acted as a partial loss-of-function mutant in microsomal preparations [8]. In this study, we measured the effect of the R14del mutant of PLN on SERCA activity for both unphosphorylated and phosphorylated PLN^{R14del} in reconstituted lipid vesicles. We found that the ΔpK_{Ca} for PLN^{R14del} is 0.17, which indicates a loss of inhibitory potency with respect to PLN^{AFA} ($\Delta pK_{Ca} = 0.26$)

(Fig. 1, A). Our data are consistent with the results obtained by Haghighi and coworkers in HEK cells [8].

The deletion of Arg14 in the cytoplasmic domain of PLN disrupts the R-R-X-S motif required for phosphorylation of Ser16 by PKA. Thus, it was predicted and shown by Young and coworkers that phosphorylation of PLN^{R14del} would be hindered. In this study, we used synthetic phosphorylation methods to determine that even upon phosphorylation of PLN^{R14del}, inhibition of SERCA is not relieved (Fig. 1, B), unlike phosphorylation of PLN^{AFA} at S16, which reverses inhibition. The pK_{Ca} for PLN^{R14del} with phosphoserine (pSer) at position 16 is virtually superimposable with the pK_{Ca} of PLN^{R14del}. This result implies that PLN^{R14del} would exert a constitutive inhibitory effect on SERCA even upon PLN^{R14del} phosphorylation by PKA, abolishing an important regulatory mechanism for the SERCA/PLN complex.

3.2. Structural dynamics of PLN^{R14del} in micelles

Our solution and solid-state NMR studies have emphasized the polymorphic behavior of PLN cytoplasmic domain [19,34], which adapts its structure to different binding partners or membrane surfaces [20,35]. The stretch of alternating hydrophobic and polar amino acids confers an amphipathic and dynamic character to the first 17 residues of PLN (Supplementary Fig. 2); establishing the structural equilibrium between the membrane-adsorbed helical T state and the solvent exposed, unfolded R state. This conformational equilibrium plays a fundamental role in Ca^{2+} homeostasis, since it regulates the extent of the ATPase inhibition and maintains SERCA activity within a physiological window. Disproportionate inhibition (super-inhibition) or complete ablation of PLN causes SERCA to function outside this window, leading to aberrant regulation of Ca^{2+} flux and progression to cardiomyopathy. Based on the previously reported high-resolution structures of PLN^{AFA} and PLN^{WT}, we predicted that the deletion of a polar residue would disrupt the amphiphilic nature of the cytoplasmic domain, reducing the interactions with the lipid membrane and promoting the unfolded, R state. To test our hypothesis, we first performed solution NMR spectroscopy to determine the effects of R14 deletion on the monomeric form of PLN^{R14del}, which carries three mutations in the transmembrane domain (C36A, C41F, and C46A) that deoligomerize the pentamer.

The [^{1}H,^{15}N]-HSQC spectrum of monomeric R14del reconstituted in DPC micelles exhibits excellent resolution of the resonances, with virtually no overlapping residues. Even the transmembrane domain residues, which are typically crowded due to the amino acid degeneracy and similar chemical environment, are fully resolved for PLN^{R14del} (Fig. 2, A). To gain initial insights into the structural behavior of R14del, we measured the chemical shift perturbations relative to PLN^{AFA} under the identical conditions (Fig. 2, B). The majority of the changes are localized near the deletion site and propagate from the juxtamembrane domain Ib to the transmembrane domain II, with Ser16 and Glu19 exhibiting the largest perturbations. These effects resemble the case of S16 phosphorylation, where the local chemical shift perturbations are associated with the unfolding of the domain Ia helix and concomitant detachment of this domain from the membrane, leading to an increase of the local flexibility [13]. To confirm that the structural changes manifested by the shift in the resonance frequencies correspond to changes in the conformational dynamics, we measured T_1, T_2 and [^{1}H,^{15}N]-NOE for the backbone amide groups. Fig. 3 shows the dimensionless parameters used to assess the extent of the mobility of the backbone atoms [36]. To place

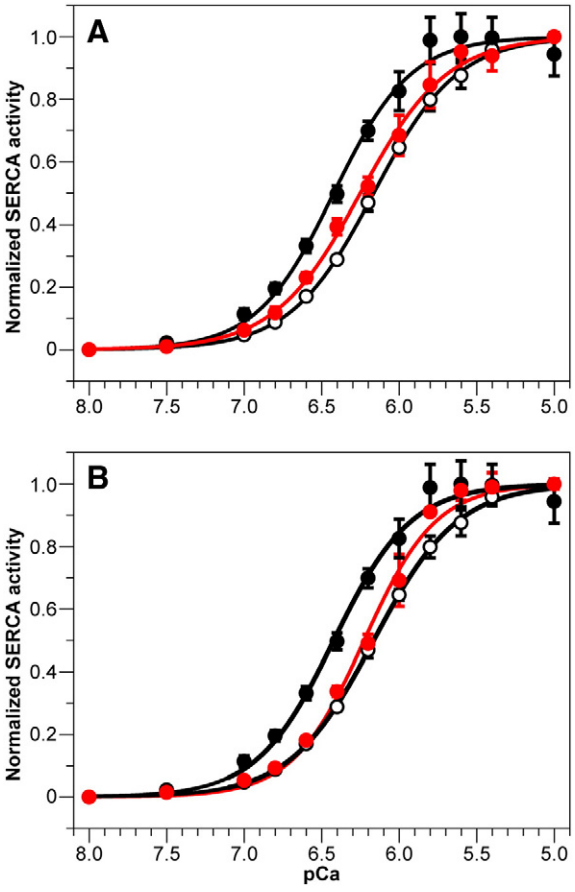

Fig. 1. ATP hydrolysis assay of SERCA alone (A and B: filled circles), in the presence of PLN^{AFA} (A and B: open circles) or R14del (red) in the non-phosphorylated state (A) or pS16 modified (B). Lipid system is multilamellar vesicles of DOPC:DOPE 4:1 (mol:mol), the lipid:SERCA:PLN molar ratio being 700:1:10. Error bars represent the standard deviation of the three measurements (see also Material and methods section).

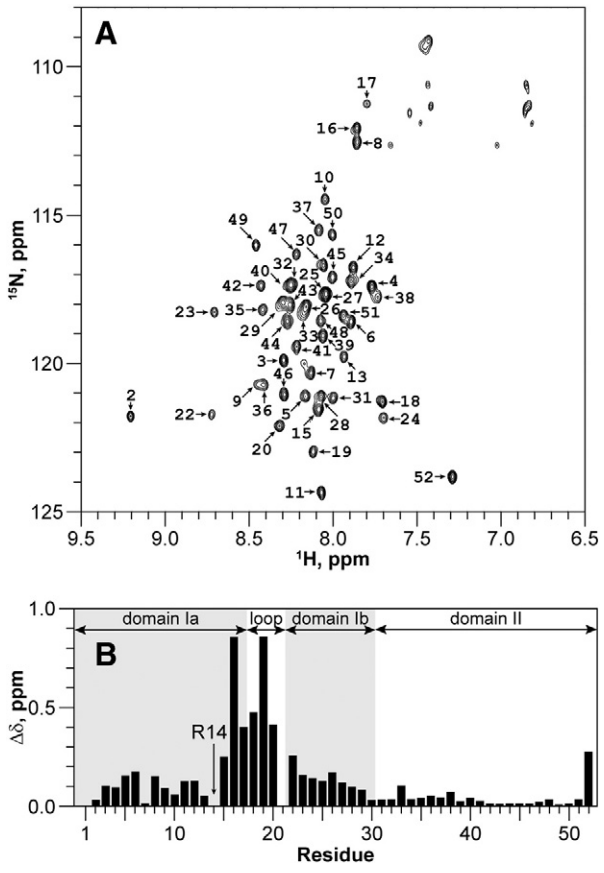

Fig. 2. HSQC spectrum of monomeric R14del in DPC-d_{38} micelles at a 450:1 detergent: protein (mol:mol). Residue numbers are indicated. Chemical shift perturbation plot relative to PLN^{AFA} in DPC-d_{38} micelles is shown as a function of the residue number.

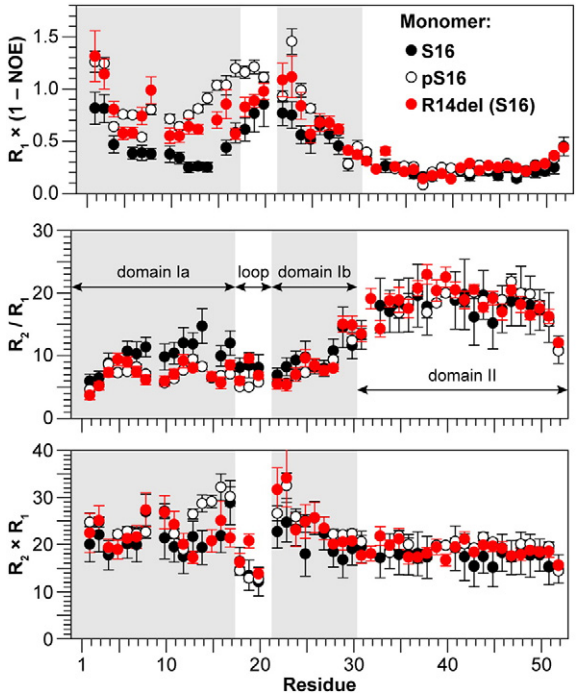

Fig. 3. Fast dynamics of R14del measured by solution NMR relaxation experiments in DPC-d_{38} micelles.

these values in context, we also include the corresponding data obtained for PLN^{AFA} both in phosphorylated and non-phosphorylated states [27,37]. The fast dynamics evaluated by the $R_1 \times (1 - \text{NOE})$ parameter show drastic changes in the cytoplasmic domain, with the most affected residues spanning positions 15–21. The increase in local motions of the cytoplasmic domain is not as extensive as for pSer16 PLN^{AFA}. The changes in motions are localized around the deletion site and appear to level off near Ala11. Since R14 deletion occurs toward the end of the cytoplasmic helix, it affects only one turn of domain Ia [38]. The remaining stretch of residues is still sufficient to form 2–3 turns of a helix, presumably stabilized by aromatic and long chain aliphatic residues that anchor this domain to the membrane [39]. Other relaxation parameters related to the motion in the μs–ms timescale can be estimated from the products or the ratios of the transverse (R_2) and longitudinal (R_1) relaxation rates. The R_2/R_1 ratios are used to assess the global correlation time and, as for PLN^{AFA}, they identify two distinct regions for the cytoplasmic and transmembrane domains. The R_2/R_1 ratios for the transmembrane domain II are identical for both monomeric and pentameric PLN since the correlation time is largely defined by the tumbling of the bulky micelle itself [40–42]. Conversely, the fast conformational dynamics of the cytoplasmic domains resemble the values obtained for pSer16 PLN^{AFA} [43]. The $R_2 \times R_1$ product for the cytoplasmic residues indicates the presence of low frequency motions near the phosphorylation site of pSer16 PLN^{AFA}, which are absent in PLN^{R14del}.

Overall, the dynamic behavior of R14del in micelles is intermediate between the inhibitory PLN^{AFA} and the non-inhibitory Ser16-phosphorylated form. The R14del mutant has enhanced dynamic behavior near the deletion site, which we attribute to local helix unwinding and detachment from the membrane. The effect is not as pronounced as for pSer16 PLN, the non-inhibitory form of PLN; nonetheless, these seemingly minor changes in the conformational dynamics of R14del affect the inhibitory potency of PLN [24,44].

3.3. Topology of PLN in oriented lipid bilayers

We previously found that the structural coupling between the membrane embedded and cytoplasmic domains is essential to PLN's inhibitory function, and altering this coupling through site-specific mutations, such as P21G, abolishes its inhibitory activity [24,38]. To understand the effects of R14 deletion on the structural coupling between the two regions of PLN, we analyzed its structural topology using oriented solid-state NMR, reconstituting the protein in oriented lipid bicelles [45]. Unlike in solution NMR, aligned solid-state NMR samples allow one to measure anisotropic properties such as chemical shift (CS) and dipolar couplings (DC) and deduce the topology of helical domains with respect to the membrane normal [46,47]. To probe the CS and DC, we used a sensitivity enhanced version of the polarization inversion spin exchange at the magic angle (or PISEMA) experiment, a separated local field experiment that correlates anisotropic chemical shifts with the dipolar couplings in oriented samples [45–47]. For the lipid bicelle, we employed a mixture of DMPC/POPC/DHPC, a composition that promotes the magnetic alignment at 25 °C. We used ytterbium ions to orient the bicelles with the lipid bilayer normal parallel to the applied magnetic field. The resonances of the membrane spanning domain of PLN^{R14del} are observed in same region of the corresponding SE-PISEMA spectrum of the PLN^{AFA} sequence (Fig. 4). The large span of the ^{15}N anisotropic chemical shifts and ^{15}N–^{1}H dipolar couplings indicate that the helical axis is tilted by approximately 30–35° with respect to the normal of the lipid bilayer. Previous studies from our group showed that the tilt angle of PLN^{WT} is dependent on the lipid bilayer thickness as well as the choice of the alignment system — mechanical or magnetic [13]. Similar behavior is observed for the monomeric species, where the tilt angle in DMPC:POPC bicelles is some 10–15° lower than the one in DOPC:DOPE glass slides. Although the tilt angle adopted by PLN^{R14del} is similar to that of PLN^{AFA}, it is possible to observe a shift in register of the resonance pattern, indicating a possible change in the azimuthal angle, although this qualitative assessment needs to be confirmed by site-specific assignments. Several resonances of the PISEMA spectrum do not follow the pattern for the well-defined helical transmembrane domain (Fig. 4, B). We detected an intense signal at 110 ppm region arising from the side chains of Asn and Gln residues as well as several backbone signals with lower intensity, resonating in the 115–125 ppm range. These latter residues must have high mobility, as signals appearing in this area correspond to near isotropic motion.

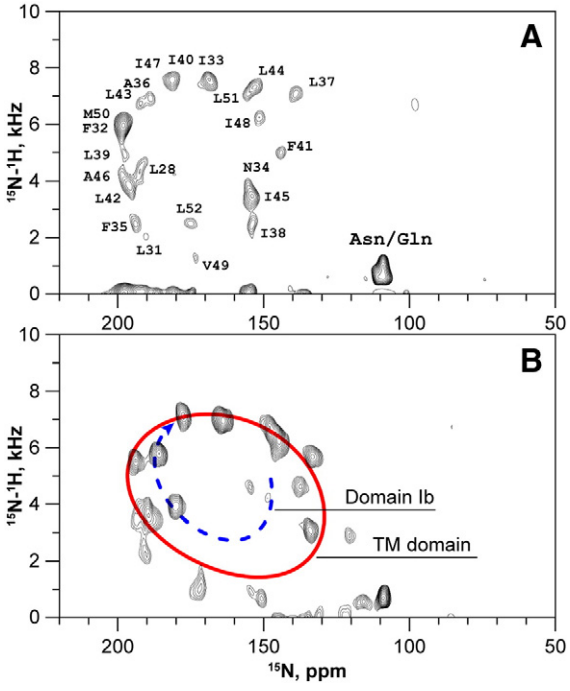

Fig. 4. SE-PISEMA spectra of PLN^{AFA} (A) and PLN^{AFA} R14del (B) in DMPC:POPC (4:1)/DHPC bicelles (q = 4.5), aligned parallel to the magnetic field. Long chained lipids to protein ratio is 130:1 (mol:mol).

The residues that do not fall within the PISA wheel of the transmembrane domain correspond to the region of PLN that is rigid and helical (blue arc in Fig. 4, B). It does not form a continuous α-helix with the rest of the membrane-spanning segment, as it would otherwise fall on the same PISA wheel (red oval in Fig. 4, B). Based on the comparison with PLN^{AFA}, we tentatively assigned these resonances to the residues located in the C-terminal part of domain Ib. This is in contrast with PLN^{AFA}, where there is a drastic reduction of signal intensity for domain Ib starting at L28 (Fig. 4, A). We tentatively assign the weak signals of PLN^{R14del} near 150 ppm and 4 kHz to Q26 and N27 located at the membrane–water interface.

The PISEMA spectrum of the R14del mutant does not show any signals corresponding to the cytoplasmic domain, which should resonate at 70–80 ppm and 3–4 kHz. Solution NMR in micelles revealed an enhanced dynamic regime of the N-terminal residues for R14del. This led us to investigate the dynamics in the native-like environment of lipid bilayers [48] with an additional technique that is exclusively sensitive toward residues that exhibit fast motions, namely magic angle spinning (MAS) spectroscopy using a refocused INEPT transfer [49,50]. To reduce the signals arising from the natural ^{13}C in lipids, we used DMPC deuterated at the acyl chains (DMPC-d_{54}). The rINEPT spectra of PLN^{AFA} (Fig. 5, A–B) show primarily the termini of the side chain groups, with distinct spectral signatures of the methyl groups as well as the ionizable side chains. In the case of R14del (Fig. 5, C–D) we detected significantly more resonances for the cytoplasmic domain with respect to the corresponding spectrum of PLN^{AFA}. The detected signals for Val, Leu, Ile, and Lys include the methylene groups of the side chains, while for Ala, Glu and Arg we observed correlations up to the backbone α-carbon. Additionally, we detected distinct C_β–H_β and C_α–H_α signals for Thr which were absent in PLN^{AFA}. The detection of signals for Thr 8 and 17 suggests that the entire cytoplasmic domain (up to domain Ib) is more mobile than PLN^{AFA}. To probe solvent accessibility for R14del, we recorded rINEPT with NOESY transfer scheme. This experiment enabled us to observe cross-peaks between the carbons of PLN and protons of water (Fig. 5, E–F). Indeed, we observe multiple side chains of R14del that are exposed to water. As expected, the ionizable moieties of Glu, Lys and Arg are all solvent exposed, suggesting that they remain charged in R14del. Additionally, we detected several aliphatic residues, namely the methyl groups of Ala, Met, Val, Leu and Ile that all show correlations with the water peak. Furthermore, the methylene group of Val and backbone of Ala and Arg are also in contact with water, which reinforces our solution NMR relaxation data and explains the lack of signals in the PISEMA experiment for the cytoplasmic residues.

3.4. Loss-of-function character of PLN^{R14del}

To further look at the R14del mutation in context with other loss-of-function (LOF) mutants, we performed analysis correlating the ^1H–^{15}N heteronuclear NOE values of the loop and domain Ib to the change in SERCA Ca^{2+} affinity induced by the presence of the mutant (Fig. 6). As previously reported, a plot of ΔpK_{Ca} versus ΔNOE yields a correlation between the structural dynamics and function, what we define as a "dynamic index" [24,44]. We have previously hypothesized that the increased dynamics of the cytoplasmic domain allows LOF PLN mutants to more readily sample excited states, pushing the populations toward the non-inhibitory B-state [19,20]. Inclusion of R14del in this structural dynamics–function correlation shows that this mutant fits the pattern

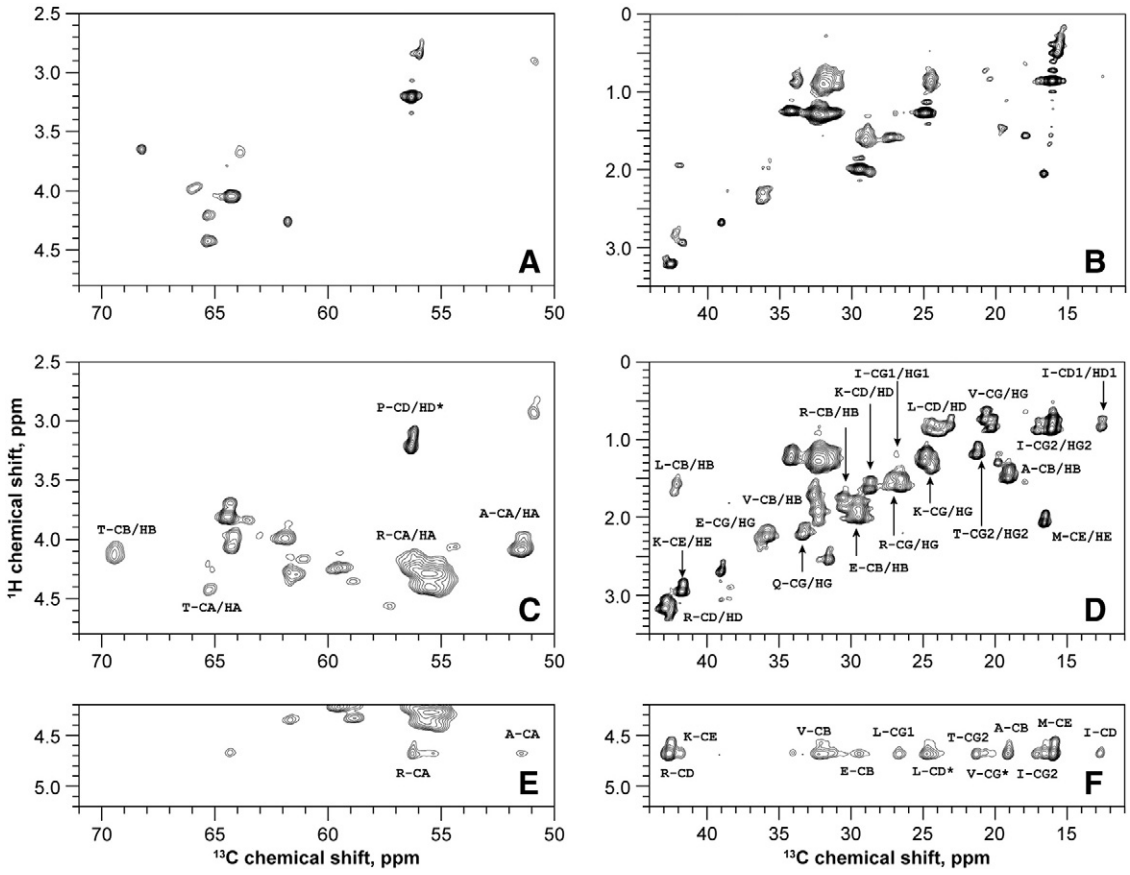

Fig. 5. Magic angle spinning spectra of PLN reconstituted in DMPC-d_{54} at 45:1 lipid:protein (mol:mol). Refocused INEPT (A–D) and NOESY-rINEPT, showing correlation with the water peak (E–F). Protein is PLN^{AFA} (A, B) or PLN^{AFA} R14del (C-F).

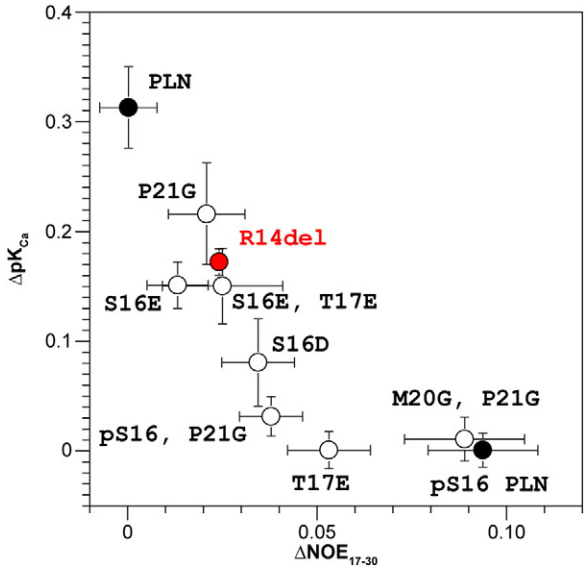

Fig. 6. Activity-dynamics correlation of PLN mutants in relation to PLN^{AFA} and PLN^{AFA} phosphorylated at Ser16 (pS16).

exhibited by the other LOF mutations which span the cytoplasmic and loop domains.

4. Discussion

In PLN^{WT} knockout mice, expression of PLN^{R14del} is cardiotoxic, with all animals carrying the R14del allele exhibiting an increased size of the heart muscle and higher mortality rates [8]. Also, contractility measurements carried out on isolated cardiomyocytes from R14del mice matched those observed in the PLN-knockout line [8,51]. In microsomal preparations, PLN^{R14del} demonstrates a loss-of-function character with respect to PLN^{WT}. However, co-expression of PLN^{WT} and R14del results in super-inhibition of SERCA, which was only partially reversed by protein kinase A phosphorylation. Based on these data, it has been proposed that the pathological nature of R14del was due to SERCA super-inhibition [8]. A possible explanation provided by these researchers was that the arginine deletion destabilized the pentameric assembly of PLN leading to de-oligomerization and increased inhibitory potency toward SERCA [8,51]. This hypothesis is supported by immunostaining data in microsomes as well as ^{32}P radiography, which showed PLN bands corresponding to lower molecular weight oligomers, although the pentameric assembly of PLN^{R14del} seems to be still present [8,51].

Phospholamban R14del has increased flexibility of the cytoplasmic domain and diminished ability to inhibit SERCA. Such features would typically render a mutant a favorable candidate for improving cardiac contractility in failing hearts, sharing similarities with the S16E, S16E–T17E, and P21G mutants of PLN [44]. Based on these factors alone, one would assume that R14del would not lead to cardiomyopathy; this implies that the dysfunction induced by this mutation is rooted in other regulatory mechanisms, such as its interactions with regulatory enzymes, including protein kinase A. The recent work from Young and co-workers shows that phosphorylation of R14del by protein kinase A is hindered [52]. This is likely due to the lack of a P-3 site necessary for protein kinase A catalytic efficiency [53–55]. Additionally, it is not possible to exclude that deletion of R14 would also cause disruption of other protein–protein interactions that characterize PLN interactome, such as A-kinase anchoring proteins (AKAPs), protein phosphatase (PP1), or CamKII kinase. PLN^{R14del} is a poor substrate for PKA since it lacks the catalytic motif needed for phosphorylation. However, we have shown here that even if a fraction of the PLN^{R14del} population is able to be phosphorylated by PKA, this will not reverse inhibition of SERCA activity. Our result explains the partial reversal of inhibition seen by Haghighi and co-workers when they co-expressed PLN^{WT} with PLN^{R14del}. We saw no relief of inhibition upon phosphorylation of Ser16 with the R14del mutant, indicating that Haghighi and co-workers measured relief of PLN^{WT} inhibition of SERCA, while PLN^{R14del} inhibition on SERCA persisted.

Solid-state NMR spectra of R14del PLN^{AFA} indicate that its inhibitory transmembrane domain mostly retains the topology of the host sequence, albeit we cannot exclude the possible change in the azimuthal angle of the transmembrane helix. The regulatory segment of PLN, harboring the arginine deletion is more mobile and not observed through cross-polarization, but can be readily detected in rINEPT spectra. Importantly, not only the side chains (which are intrinsically more mobile) can be seen in R14del rINEPT, but several backbone signals are detected as well. NOESY transfer between R14del and water illustrates that the cytoplasmic domain is solvated, suggesting that the conformational equilibrium of R14del is shifted toward the unfolded, membrane-detached R-state. The dissociation of the cytoplasmic domain from the membrane is likely a combination of several factors. First, the wild type sequence is itself polymorphic, adopting several structural states. Therefore, changes in the primary sequence may shift the structural equilibrium toward a specific state. While several amphipathic peptides are unstructured in water and fold in the presence of the lipid bilayer [56], this is not the case for PLN's cytoplasmic domain. Second, elimination of the ionized residue can weaken electrostatic interactions of the protein with the lipid headgroups [57]. Third, a deletion of a residue in the amphipathic segment has an effect of changing the amino acid register on the helical wheel, interspersing the hydrophobic and hydrophilic side chains. Several studies have shown that such mutations can alter the structure and/or topology of the peptides [58]. Based on these considerations, we anticipate that the naturally occurring PLN mutations at Arg9 to a hydrophobic residue may have a similar effect, with the regulatory cytoplasmic domain of the R9X mutants exhibiting altered dynamics relative to the wild type.

5. Conclusions

Using solution and solid-state NMR methods, we analyzed the structural dynamics and topology of the R14del mutation in correlation with SERCA ATPase assays. While R14del is related to the development of cardiomyopathy, the structural and dynamic features of this mutant correlate with the structure–dynamics–function relationship that we previously identified for several loss-of-function PLN mutants that relieve SERCA inhibition. These results reveal that in an isolated system, removal of the Arg14 residue renders PLN a less potent inhibitor of SERCA. Interestingly, phosphorylation of PLN^{R14del} at Ser16 does not relieve inhibition and mimics the functional behavior of pSer16 PLN. Considering that the increased dynamics observed by NMR and the diminished SERCA inhibition would lead to an increase in SERCA activity and possibly cardiac contractility, the deleterious physiological consequences of the R14 deletion appear to be comprised of a variety of mechanisms, some of which are dependent on proteins involved in the tight interplay that occurs during calcium signaling. Because of the location of the mutation within the recognition sequence of these enzymes, likely binding partners of PLN that are directly affected by the deletion of Arg14 are protein kinase A and protein phosphatase I. These proteins are central to maintain phosphorylation levels and Ca^{2+} transport within the physiological range.

Note added in proof

After the submission of the revised manuscript, Hughes and Middleton also reported on the enhanced conformational dynamics of PLNR14del (PLOS One, e106746).

Acknowledgements

This work is supported by a grant from the National Institute of Health (GM072701) and fellowships from the American Heart Association (13POST14670054 to V.V. and 13PRE16950023 to K.S.) and the National Heart Lung and Blood Institute (5F31HL095361 to K.H.). The NMR spectra were acquired at the Minnesota NMR Center. G.V., V.V., K.S., K.H. and T.G. designed and performed the experiments. V.V. and K.S. analyzed the data. V.V. and G.V. wrote the manuscript with input from K.S., K.H., and T.G.

Appendix A. Supplementary data

Supplementary data to this article can be found online at http://dx.doi.org/10.1016/j.bbamem.2014.09.007.

References

[1] L. Dellefave, E.M. McNally, The genetics of dilated cardiomyopathy, Curr. Opin. Cardiol. 25 (2010) 198–204.
[2] R.E. Hershberger, D.J. Hedges, A. Morales, Dilated cardiomyopathy: the complexity of a diverse genetic architecture, Nat. Rev. Cardiol. 10 (2013) 531–547.
[3] D.H. MacLennan, Y. Kimura, T. Toyofuku, Sites of regulatory interaction between calcium ATPases and phospholamban, Ann. N. Y. Acad. Sci. 853 (1998) 31–42.
[4] H.S. Wang, D.A. Arvanitis, M. Dong, P.J. Niklewski, W. Zhao, C.K. Lam, E.G. Kranias, D. Sanoudou, SERCA2a superinhibition by human phospholamban triggers electrical and structural remodeling in mouse hearts, Physiol. Genomics 43 (2011) 357–364.
[5] R. Parvari, A. Levitas, The mutations associated with dilated cardiomyopathy, Biochem. Res. Int. 2012 (2012) 639250.
[6] K. Haghighi, F. Kolokathis, L. Pater, R.A. Lynch, M. Asahi, A.O. Gramolini, G.C. Fan, D. Tsiapras, H.S. Hahn, S. Adamopoulos, S.B. Liggett, G.W. Dorn II, D.H. MacLennan, D.T. Kremastinos, E.G. Kranias, Human phospholamban null results in lethal dilated cardiomyopathy revealing a critical difference between mouse and human, J. Clin. Invest. 111 (2003) 869–876.
[7] J.P. Schmitt, M. Kamisago, M. Asahi, G.H. Li, F. Ahmad, U. Mende, E.G. Kranias, D.H. MacLennan, J.G. Seidman, C.E. Seidman, Dilated cardiomyopathy and heart failure caused by a mutation in phospholamban, Science 299 (2003) 1410–1413.
[8] K. Haghighi, F. Kolokathis, A.O. Gramolini, J.R. Waggoner, L. Pater, R.A. Lynch, G.C. Fan, D. Tsiapras, R.R. Parekh, G.W. Dorn II, D.H. MacLennan, D.T. Kremastinos, E.G. Kranias, A mutation in the human phospholamban gene, deleting arginine 14, results in lethal, hereditary cardiomyopathy, Proc. Natl. Acad. Sci. U. S. A. 103 (2006) 1388–1393.
[9] A. Medeiros, D.G. Biagi, T.J. Sobreira, P.S. de Oliveira, C.E. Negrao, A.J. Mansur, J.E. Krieger, P.C. Brum, A.C. Pereira, Mutations in the human phospholamban gene in patients with heart failure, Am. Heart J. 162 (2011) 1088–1095.
[10] P.A. van der Zwaag, I.A. van Rijsingen, A. Asimaki, J.D. Jongbloed, D.J. van Veldhuisen, A.C. Wiesfeld, M.G. Cox, L.T. van Lochem, R.A. de Boer, R.M. Hofstra, I. Christiaans, K. Y. van Spaendonck-Zwarts, R.H. Lekanne dit Deprez, D.P. Judge, H. Calkins, A.J. Suurmeijer, R.N. Hauer, J.E. Saffitz, A.A. Wilde, M.P. van den Berg, J.P. van Tintelen, Phospholamban R14del mutation in patients diagnosed with dilated cardiomyopathy or arrhythmogenic right ventricular cardiomyopathy: evidence supporting the concept of arrhythmogenic cardiomyopathy, Eur. J. Heart Fail. 14 (2012) 1199–1207.
[11] M. Tada, M.A. Kirchberger, A.M. Katz, Phosphorylation of a 22,000-dalton component of the cardiac sarcoplasmic reticulum by adenosine 3′:5′-monophosphate-dependent protein kinase, J. Biol. Chem. 250 (1975) 2640–2647.
[12] H. Ghimire, S. Abu-Baker, I.D. Sahu, A. Zhou, D.J. Mayo, R.T. Lee, G.A. Lorigan, Probing the helical tilt and dynamic properties of membrane-bound phospholamban in magnetically aligned bicelles using electron paramagnetic resonance spectroscopy, Biochim. Biophys. Acta 1818 (2012) 645–650.
[13] V.V. Vostrikov, K.R. Mote, R. Verardi, G. Veglia, Structural dynamics and topology of phosphorylated phospholamban homopentamer reveal its role in the regulation of calcium transport, Structure 21 (2013) 2119–2130.
[14] R. Verardi, L. Shi, N.J. Traaseth, N. Walsh, G. Veglia, Structural topology of phospholamban pentamer in lipid bilayers by a hybrid solution and solid-state NMR method, Proc. Natl. Acad. Sci. U. S. A. 108 (2011) 9101–9106.
[15] R.L. Cornea, J.M. Autry, Z. Chen, L.R. Jones, Reexamination of the role of the leucine/isoleucine zipper residues of phospholamban in inhibition of the Ca^{2+} pump of cardiac sarcoplasmic reticulum, J. Biol. Chem. 275 (2000) 41487–41494.
[16] C. Toyoshima, S. Iwasawa, H. Ogawa, A. Hirata, J. Tsueda, G. Inesi, Crystal structures of the calcium pump and sarcolipin in the Mg^{2+}-bound E1 state, Nature 495 (2013) 260–264.
[17] A.M. Winther, M. Bublitz, J.L. Karlsen, J.V. Moller, J.B. Hansen, P. Nissen, M.J. Buch-Pedersen, The sarcolipin-bound calcium pump stabilizes calcium sites exposed to the cytoplasm, Nature 495 (2013) 265–269.
[18] B.L. Akin, T.D. Hurley, Z. Chen, L.R. Jones, The structural basis for phospholamban inhibition of the calcium pump in sarcoplasmic reticulum, J. Biol. Chem. 288 (2013) 30181–30191.
[19] M. Gustavsson, N.J. Traaseth, G. Veglia, Probing ground and excited states of phospholamban in model and native lipid membranes by magic angle spinning NMR spectroscopy, Biochim. Biophys. Acta 1818 (2012) 146–153.
[20] M. Gustavsson, R. Verardi, D.G. Mullen, K.R. Mote, N.J. Traaseth, T. Gopinath, G. Veglia, Allosteric regulation of SERCA by phosphorylation-mediated conformational shift of phospholamban, Proc. Natl. Acad. Sci. U. S. A. 110 (2013) 17338–17343.
[21] L.R. Jones, R.L. Cornea, Z. Chen, Close proximity between residue 30 of phospholamban and cysteine 318 of the cardiac Ca^{2+} pump revealed by intermolecular thiol cross-linking, J. Biol. Chem. 277 (2002) 28319–28329.
[22] C. Toyoshima, M. Asahi, Y. Sugita, R. Khanna, T. Tsuda, D.H. MacLennan, Modeling of the inhibitory interaction of phospholamban with the Ca^{2+} ATPase, Proc. Natl. Acad. Sci. U. S. A. 100 (2003) 467–472.
[23] K. Seidel, O.C. Andronesi, J. Krebs, C. Griesinger, H.S. Young, S. Becker, M. Baldus, Structural characterization of Ca^{2+}-ATPase-bound phospholamban in lipid bilayers by solid-state nuclear magnetic resonance (NMR) spectroscopy, Biochemistry 47 (2008) 4369–4376.
[24] K.N. Ha, N.J. Traaseth, R. Verardi, J. Zamoon, A. Cembran, C.B. Karim, D.D. Thomas, G. Veglia, Controlling the inhibition of the sarcoplasmic Ca^{2+}-ATPase by tuning phospholamban structural dynamics, J. Biol. Chem. 282 (2007) 37205–37214.
[25] J. Radoicic, G.J. Lu, S.J. Opella, NMR structures of membrane proteins in phospholipid bilayers, Q. Rev. Biophys. 47 (2014) 249–283.
[26] B. Buck, J. Zamoon, T.L. Kirby, T.M. DeSilva, C. Karim, D. Thomas, G. Veglia, Overexpression, purification, and characterization of recombinant Ca-ATPase regulators for high-resolution solution and solid-state NMR studies, Protein Expr. Purif. 30 (2003) 253–261.
[27] E.E. Metcalfe, J. Zamoon, D.D. Thomas, G. Veglia, $^{1}H/^{15}N$ heteronuclear NMR spectroscopy shows four dynamic domains for phospholamban reconstituted in dodecylphosphocholine micelles, Biophys. J. 87 (2004) 1205–1214.
[28] E.A. Morrison, K.A. Henzler-Wildman, Reconstitution of integral membrane proteins into isotropic bicelles with improved sample stability and expanded lipid composition profile, Biochim. Biophys. Acta 1818 (2012) 814–820.
[29] R.S. Prosser, S.A. Hunt, J.A. DiNatale, R.R. Vold, Magnetically aligned membrane model systems with positive order parameter: switching the sign of S_{zz} with paramagnetic ions, J. Am. Chem. Soc. 118 (1996) 269–270.
[30] D.L. Stokes, N.M. Green, Three-dimensional crystals of CaATPase from sarcoplasmic reticulum. Symmetry and molecular packing, Biophys. J. 57 (1990) 1–14.
[31] L.G. Reddy, R.L. Cornea, D.L. Winters, E. McKenna, D.D. Thomas, Defining the molecular components of calcium transport regulation in a reconstituted membrane system, Biochemistry 42 (2003) 4585–4592.
[32] T.D. Madden, D. Chapman, P.J. Quinn, Cholesterol modulates activity of calcium-dependent ATPase of the sarcoplasmic reticulum, Nature 279 (1979) 538–541.
[33] M. Gustavsson, N.J. Traaseth, G. Veglia, Activating and deactivating roles of lipid bilayers on the Ca^{2+}-ATPase/phospholamban complex, Biochemistry 50 (2011) 10367–10374.
[34] C.B. Karim, T.L. Kirby, Z. Zhang, Y. Nesmelov, D.D. Thomas, Phospholamban structural dynamics in lipid bilayers probed by a spin label rigidly coupled to the peptide backbone, Proc. Natl. Acad. Sci. U. S. A. 101 (2004) 14437–14442.
[35] L.R. Masterson, T. Yu, L. Shi, Y. Wang, M. Gustavsson, M.M. Mueller, G. Veglia, cAMP-dependent protein kinase A selects the excited state of the membrane substrate phospholamban, J. Mol. Biol. 412 (2011) 155–164.
[36] V.A. Jarymowycz, M.J. Stone, Fast time scale dynamics of protein backbones: NMR relaxation methods, applications, and functional consequences, Chem. Rev. 106 (2006) 1624–1671.
[37] E.E. Metcalfe, N.J. Traaseth, G. Veglia, Serine 16 phosphorylation induces an order-to-disorder transition in monomeric phospholamban, Biochemistry 44 (2005) 4386–4396.
[38] N.J. Traaseth, L. Shi, R. Verardi, D.G. Mullen, G. Barany, G. Veglia, Structure and topology of monomeric phospholamban in lipid membranes determined by a hybrid solution and solid-state NMR approach, Proc. Natl. Acad. Sci. U. S. A. 106 (2009) 10165–10170.
[39] K.A. Sparks, N.J. Gleason, R. Gist, R. Langston, D.V. Greathouse, R.E. Koeppe II, Comparisons of interfacial Phe, Tyr, and Trp residues as determinants of orientation and dynamics for GWALP transmembrane peptides, Biochemistry 53 (2014) 3637–3645.
[40] V.V. Vostrikov, H. Gu, H.I. Ingolfsson, J.F. Hinton, O.S. Andersen, B. Roux, R.E. Koeppe II, Gramicidin A backbone and side chain dynamics evaluated by molecular dynamics simulations and nuclear magnetic resonance experiments. II: nuclear magnetic resonance experiments, J. Phys. Chem. B 115 (2011) 7427–7432.
[41] L.N. de Medeiros, R. Angeli, C.G. Sarzedas, E. Barreto-Bergter, A.P. Valente, E. Kurtenbach, F.C. Almeida, Backbone dynamics of the antifungal Psd1 pea defensin and its correlation with membrane interaction by NMR spectroscopy, Biochim. Biophys. Acta 1798 (2010) 105–113.
[42] R.C. Oliver, J. Lipfert, D.A. Fox, R.H. Lo, S. Doniach, L. Columbus, Dependence of micelle size and shape on detergent alkyl chain length and head group, PLoS One 8 (2013) e62488.
[43] C.B. Anfinsen, Principles that govern the folding of protein chains, Science 181 (1973) 223–230.
[44] K.N. Ha, M. Gustavsson, G. Veglia, Tuning the structural coupling between the transmembrane and cytoplasmic domains of phospholamban to control sarcoplasmic reticulum Ca^{2+}-ATPase (SERCA) function, J. Muscle Res. Cell Motil. 33 (2012) 485–492.
[45] T. Gopinath, G. Veglia, Sensitivity enhancement in static solid-state NMR experiments via single- and multiple-quantum dipolar coherences, J. Am. Chem. Soc. 131 (2009) 5754–5756.
[46] F.M. Marassi, S.J. Opella, A solid-state NMR index of helical membrane protein structure and topology, J. Magn. Reson. 144 (2000) 150–155.

[47] J. Wang, J. Denny, C. Tian, S. Kim, Y. Mo, F. Kovacs, Z. Song, K. Nishimura, Z. Gan, R. Fu, J.R. Quine, T.A. Cross, Imaging membrane protein helical wheels, J. Magn. Reson. 144 (2000) 162–167.
[48] H.X. Zhou, T.A. Cross, Influences of membrane mimetic environments on membrane protein structures, Annu. Rev. Biophys. 42 (2013) 361–392.
[49] O.C. Andronesi, S. Becker, K. Seidel, H. Heise, H.S. Young, M. Baldus, Determination of membrane protein structure and dynamics by magic-angle-spinning solid-state NMR spectroscopy, J. Am. Chem. Soc. 127 (2005) 12965–12974.
[50] D.M. Thomas, M.R. Bendall, D.T. Pegg, D.M. Doddrell, J. Field, Two-dimensional ^{13}C–^{1}H polarization transfer *J* spectroscopy, J. Magn. Reson. 42 (1981) 298–306.
[51] K. Haghighi, T. Pritchard, J. Bossuyt, J.R. Waggoner, Q. Yuan, G.C. Fan, H. Osinska, A. Anjak, J. Rubinstein, J. Robbins, D.M. Bers, E.G. Kranias, The human phospholamban Arg14-deletion mutant localizes to plasma membrane and interacts with the Na/K-ATPase, J. Mol. Cell. Cardiol. 52 (2012) 773–782.
[52] D.K. Ceholski, C.A. Trieber, C.F. Holmes, H.S. Young, Lethal, hereditary mutants of phospholamban elude phosphorylation by protein kinase A, J. Biol. Chem. 287 (2012) 26596–26605.
[53] D. Kubler, W. Pyerin, O. Bill, A. Hotz, J. Sonka, V. Kinzel, Evidence for ecto-protein kinase activity that phosphorylates Kemptide in a cyclic AMP-dependent mode, J. Biol. Chem. 264 (1989) 14549–14555.
[54] O. Zetterqvist, U. Ragnarsson, E. Humble, L. Berglund, L. Engstrom, The minimum substrate of cyclic AMP-stimulated protein kinase, as studied by synthetic peptides representing the phosphorylatable site of pyruvate kinase (type L) of rat liver, Biochem. Biophys. Res. Commun. 70 (1976) 696–703.
[55] J.A. Adams, S.S. Taylor, Phosphorylation of peptide substrates for the catalytic subunit of cAMP-dependent protein kinase, J. Biol. Chem. 268 (1993) 7747–7752.
[56] D.I. Fernandez, M.A. Sani, A.J. Miles, B.A. Wallace, F. Separovic, Membrane defects enhance the interaction of antimicrobial peptides, aurein 1.2 versus caerin 1.1, Biochim. Biophys. Acta 1828 (2013) 1863–1872.
[57] J. Georgescu, V.H. Munhoz, B. Bechinger, NMR structures of the histidine-rich peptide LAH_4 in micellar environments: membrane insertion, pH-dependent mode of antimicrobial action, and DNA transfection, Biophys. J. 99 (2010) 2507–2515.
[58] S. Fanghanel, P. Wadhwani, E. Strandberg, W.P. Verdurmen, J. Burck, S. Ehni, P.K. Mykhailiuk, S. Afonin, D. Gerthsen, I.V. Komarov, R. Brock, A.S. Ulrich, Structure analysis and conformational transitions of the cell penetrating peptide transportan 10 in the membrane-bound state, PLoS One 9 (2014) e99653.